Study of Passive Chipless IR-UWB Indoor Positioning Based on Time-of-Arrival and Band-Notch

Jian Liu

School of Communication and Information Engineering
Xi'an University of Science and Technology, Xi'an, 710054, China
Liujian02@xust.edu.cn

Abstract ─ In the paper, a passive and chipless IR-UWB indoor positioning system is proposed that follows the criteria of spectral and temporal joint identification. In the scenario of a 2D positioning, the system is coordinated by three anchors; a node can then be positioned by recognizing the pulse's time-of-arrival (TOA) and the pulse's band-notch in its backscattered spectrum. The model of the positioning system is established and the numerical analysis is committed in terms of a conceived positioning example. Results validate the system that the positioning is accurate, and the accuracy can be further improved by calibrating the value of TOA through the time offset made by the pulses backscattered by the anchor with and without band-notch, respectively.

Index Terms ─ Band-notch, indoor positioning, IR-UWB, TOA.

I. INTRODUCTION

Indoor positioning is quite necessary in many fields such as the healthcare where tracking human body and limbs movement is required [1]. Compared with outdoor, the indoor positioning is very difficult because the channel is more easily influenced by the phenomenon of reflection or dispersion. In the recent years, people began to seek solution in the field of transient electromagnetism, considering of the transient field can render radio signal be more constraint in time domain. Research has demonstrated that short pulses can be really effective in avoiding channel deterioration and system noise, so as to make positioning be accurate at least for the system where positioning is mainly depending on the value of time-of-arrival (TOA).

One specification for the application of transient electromagnetic field is the ultra-wideband (UWB) that was released in 2002 by the Federal Communications Commission (FCC) for the unlicensed frequency band (from 3.1 GHz to 10.6 GHz) used for the short range communication. Nowadays, the UWB has increasingly become a substitution for the traditional narrow band circumstance in the area of radio frequency identification (RFID). The UWB enabled RFID (UWB-RFID) is recognized as a more advanced architecture used for the identification or the localization of an object in a very short range area [2-4].

In theory, the ultra-wideband (UWB) refers to the radio with a bandwidth exceeding the lesser of 500 MHz or 20% of the arithmetic center frequency. The UWB signal in time domain is therefore a very constraint pulse shortened in nanosecond, usually known as the Impulse Radio Ultra-Wideband (IR-UWB) [5]. It is the shortness of the pulse that can readily render IR-UWB positioning be accurate, and the accuracy can be improved further by employing shorter, more precise pulse with higher level of integrity. It's sure a good solution in this regards, but it also brings about a lot of critical technical problems, for example, the shorter pulses have to make the realization of clock jitter or the retrieving of critical parameters from pulse's figure become quite difficult [6].

Nevertheless, there are still some efforts had been dedicated to this area [7-10]. For example in [11], a uni-planar monopole antenna is proposed that is made by a passive and chipless IR-UWB tag, committing to positioning based on the parameters contained in the antenna modem and controlled by the length of meandrous coplanar waveguide plane (CWP) loaded, respectively, by impedance match circuit, open circuit and short circuit. The location and the polarity of the late-time pulse correlated by the pulse received by the object for positioning (node) in early time become the rule governing the whole procedure of positioning.

Although the example comes forth a very simple and easy implementation for positioning in accordance with the modem of antenna mode (In the theory of transient field, the wave backscattered by antenna is composed of two modes, one is called the structural mode, another is called the antenna mode), it has no way to offer clues to make anchor be clearly identified, although in some circumstance, this parameter or value are indispensable [12]. So, in this paper, we design and develop a positioning system based on the IR-UWB architecture that is novel enough in the aspect of the recognition of pulse and the corresponding anchor solely depending on the feature of anchor's band-notch. We

Submitted On: September 18, 2017
Accepted On: April 21, 2018

focus on the 2D positioning; therefore the positioning system is coordinated by three anchors that are the sort of passive and chipless IR-UWB tag decorated with different band-notches. A node can be positioned and scaled on account of them through retrieving and analyzing the feature of pulse both in the temporal (TOA) and in the spectral domain (band-notch).

The reminders of the paper are: the IR-UWB positioning system for the 2D application is firstly introduced in Section II with interpretation of the exact algorithm and criteria of positioning. Secondly, the topology of anchor and node are illustrated with the details of the geometric dimensions shown in Section III. Thirdly, the procedure, analyzing, calibrating are described by a complete analysis of each result in Section IV. Finally, the conclusions are made in Section V.

II. THE ARCHITECTURE OF PASSIVE AND CHIPLESS IR-UWB POSITIONING SYSTEM

The coordinate of the proposed positioning system in terms of the 2D scenario is the Cartesian where a node can be scaled and benchmarked by three anchors that are distributed orthogonally each other, as shown in Fig. 1. According to the theory of IR-UWB, all the anchors are the sort of passive and chipless tags, functioning to make impinging pulse backscatter to node. The node is, however, an object for positioning that is an active and chip-have UWB-RFID tag for instead. In a specific positioning, the node works to transmitting a UWB pulse to anchors, and then receives the backscattered copy of them. As a result, the exact position of the node can be determined by retrieving and analyzing the TOA and the band-notch feature borne in the backscattered structural mode.

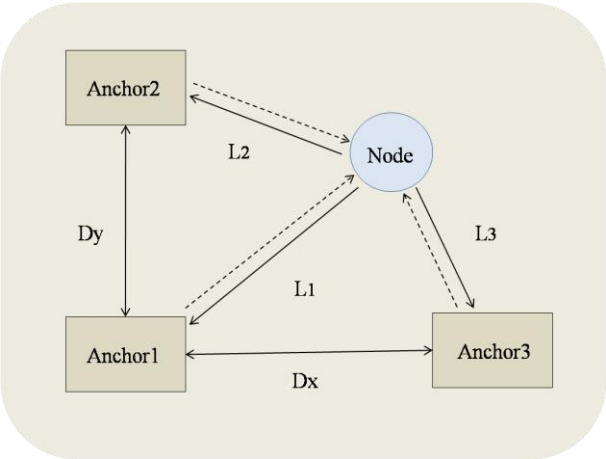

Fig. 1. The model of the passive and chipless IR-UWB positioning system.

A. Positioning model

The Cartesian is coordinated by three anchors known as anchor1, anchor2 and anchor3, as shown in Fig. 1. The horizontal line linking the anchor1 and the anchor3 forms the *x* axial scaled by *Dx*, denoting the distance between the anchor1 and the anchor3. The vertical line linking the anchor1 and the anchor2 forms the *y* axial scaled by *Dy* that denotes the distance between the anchor1 and the anchor2. If one node is assumed to be placed at (*x*, *y*), L_1, L_2 and L_3 are used to represent the distances from the node to the anchor1, the anchor2 and the anchor3, respectively.

B. Positioning algorithm

The positioning algorithm is configured in terms of the system that is based on the temporal and spectral joint identification. Referring to the model illustrated in Fig. 1, the coordinate (*x*, *y*) of a node can be determined by:

$$\begin{cases} x = \left[D_x^2 - \left(L_3^2 - L_1^2 \right) \right] \Big/ 2D_x \\ y = \left[D_y^2 - \left(L_2^2 - L_1^2 \right) \right] \Big/ 2D_y \end{cases}, \tag{1}$$

in which, $L_1=t_1/2c$, $L_2=t_2/2c$, $L_3=t_3/2c$; t_1, t_2 , t_3 are the TOA at node after being backscattered by the anchor1, the anchor2 and the anchor3, respectively; *c* is the velocity of pulse travelling in free space.

It is evidence that TOA in the algorithm isn't sufficient to issue a positioning alone. On the contrary, it is quite necessary to know the pulse and the corresponding anchor that the pulse is backscattered. So, there shall be an assumption hindered in the algorithm that anchor can be virtually identified by the band-notch of the pulse in the backscattered spectrum. The algorithm plus the hindered assumption will determine the configurations of both the node and the anchor simultaneously.

III. THE CONFIGURATION OF ANCHOR AND NODE

A. Node topology

Node is the object-for-positioning. Under the architecture of IR-UWB, the node shall be facilitate to transmitting and receiving UWB signals, and then give them an analysis. So, the topology of the node shall be constructed by two parts: one is the antenna covering UWB band, another is the digital processing unit (IC chipset) used for launching the algorithm of positioning. To make the node simple in structure, the UWB antenna is configured specifically by a planar metallic patch decorated by symmetric double concaved angles, as shown in Fig. 2 (a). The positioning unit is connected to the antenna through a microstrip line. The dimension of the topology of the node are listed in Table1 that make the node satisfy for the specifications of UWB with frequency range from 3.1 GHz to 10.6 GHz [13].

Table 1: Dimension of anchor and node (Unit:mm)

Symbol	Value	Definition
Wp	18.6	Width of rectangular patch
Hp	15.5	Height of rectangular patch
Hc	1.5	Height of staircase 1
Hd	1.5	Height of staircase 2
Wc	1.5	Width of staircase 1
Wd	1.5	Width of staircase 2
Hg	10.4	Height of grounding plane
Hf	11.0	Height of microstrip line

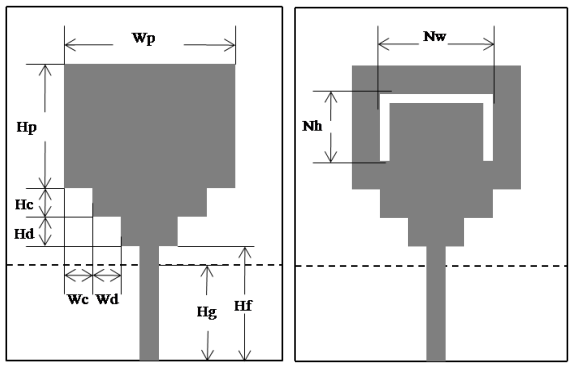

Fig. 2. The topology of node (a) and anchor (b).

B. Anchor topology

Anchors fabricate the coordinate of the positioning system. Under the architecture of IR-UWB, the anchors function to make positioning pulse be backscattered while leaves only the structural mode there. So, the topology of the anchor shall be constructed by a passive and chipless UWB tag equipped with an UWB antenna and an impedance match load (usually 50 Ohm resistance). In addition, a U-slot is etched on the facet of the antenna on each anchor [14], as shown in Fig. 2 (b). Study has shown that the U-slot can give anchor a band-notch in the spectrum of the backscattered structural mode [15-17]. In terms of 2D positioning, three anchors are need, each is borne with different band-notch. The lengths of U-slot attached to each anchor are listed in Table 2.

Table 2: Length of U-slot on anchor (Unit:mm)

Symbol	Anchor1	Anchor2	Anchor3
Nw	12.0	10.0	9.0
Nh	8.0	7.0	6.5

IV. POSITIONING PROCEDURE, ANAYZING AND CALIBRATION

The positioning signal is set by a Gaussian pulse as shown in Fig. 3. Since the anchors are all impedance match, the pulses backscattered by anchors are only the structural modes, as shown in Fig. 4.

Figure 5 (b) shows the spectrum of the structural modes backscattered by anchors with different U-slots. Compared with the pulse that is presumed to be backscattered by the anchor with the same size, without band-notch as shown in Fig. 5 (a), the anchor1 can be determined to have a band-notch at 5.26 GHz, the anchor2 has band-notch at 5.94 GHz, and the anchor3 has a band-notch at 6.49 GHz.

A. Positioning procedure

The positioning procedure is illustrated, assuming a node is placed at (60, 80) mm. When the pulse shown in Fig. 3 is transmitted by the node, it will impinge to the anchor1 and be backscattered. The pulse reaching at the node is the pulse as shown in Fig. 6. According to the algorithm, the TOA of the pulse can be determined by the time of the peak of the pulse with correspondence to the time interval. The peak of the pulse from the anchor1 is at the time of 0.8452ns. Compared with the peak of the pulse transmitted by the node at the time of 0.4405ns, the time interval in between is 0.4047ns, representing that the distance between the anchor1 and the node is 101.41mm (L_1). Likewise, Fig. 7 shows the pulse backscattered by the anchor2 and arrived at the node. The peak of the pulse from the anchor2 is at the time of 0.7214ns. Compared with the peak of the pulse transmitted by the node at the time of 0.4405ns, the time interval is 0.2809ns, indicating that the distance between the anchor2 and the node is 64.27mm (L_2). Similarly, Fig. 8 shows the pulse backscattered by the anchor3 and arrived at the node. The peak of the pulse from anchor3 is at the time of 0.8066ns. Compared with the peak of the pulse transmitted by the node at the time of 0.4405ns, the time interval is 0.3661ns, denoting the distance between the anchor3 and the node is 89.93mm (L_3).

Using the Equation (1), the position of the node can be determined by the coordinate of (60.94, 80.79) mm. The result shows that the deviation of the positioning in the horizontal direction is about 0.94mm; but in the vertical direction, the deviation is 0.79mm.

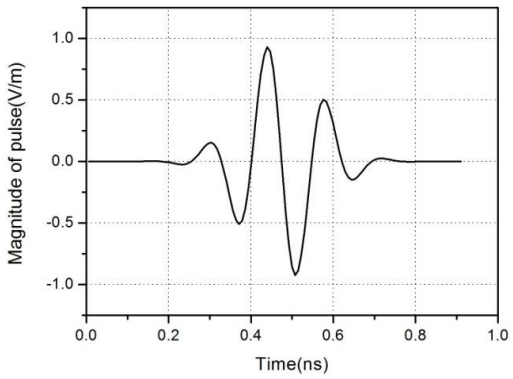

Fig. 3. Ultra-wideband Gaussian pulse used for positioning.

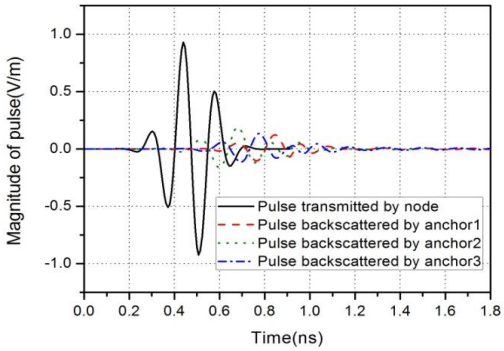

Fig. 4. Pulses (structural mode) backscattered by anchors and arrived at node.

B. Positioning calibration

Since the introduction of U-slot into anchor's facet, it is certainty that the pulse backscattered there will be distorted somewhat compared with that from the anchor not be equipped with U-slot. Through numerical analysis, we can show that the distortion of the pulse backscattered by the anchor1 is as illustrated in Fig. 9. The time offset at the peak of the pulse is 0.00349ns. This offset can be used to calibrate the exactness of the TOA in terms of the pulse backscattered by the anchor1. The TOA after being calibrated is turned to 0.8417ns; and accordingly, the distance (L_1) is revised to 100.36mm [18].

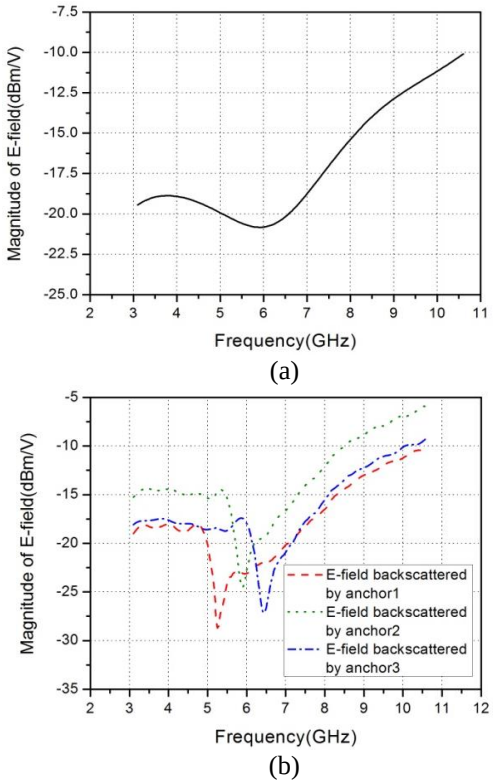

Fig. 5. Spectrum of pulses: (a) for anchor without band-notch; (b) for three anchors with different band notches.

In Fig. 10, the time offset caused by the anchor2 is 0.00247ns. The TOA after being calibrated is changed to 0.7189ns; and accordingly, the distance (L_2) is revised to 63.53mm.

Similarly, in Fig. 11, the time offset caused by the anchor3 is 0.00002ns, the TOA after being calibrated is to be 0.80662ns; and accordingly, the distance (L_3) can be revised to 89.84mm.

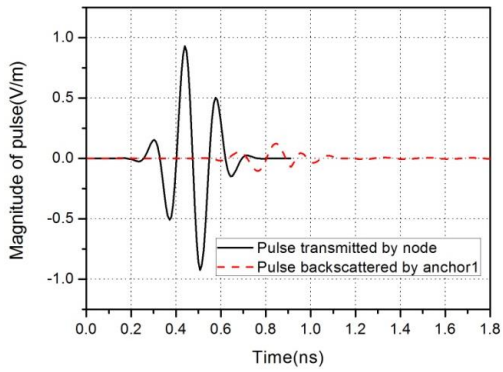

Fig. 6. Pulse backscattered by anchor1 compared with that transmitted by node.

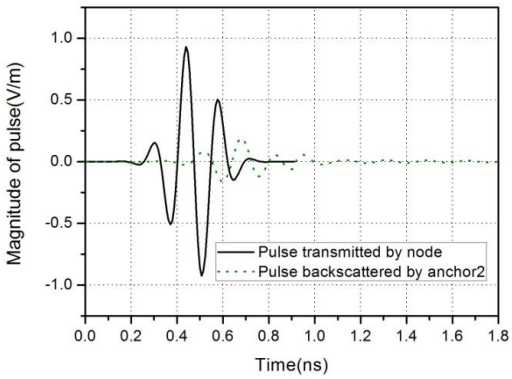

Fig. 7. Pulse backscattered by anchor2 compared with that transmitted by node.

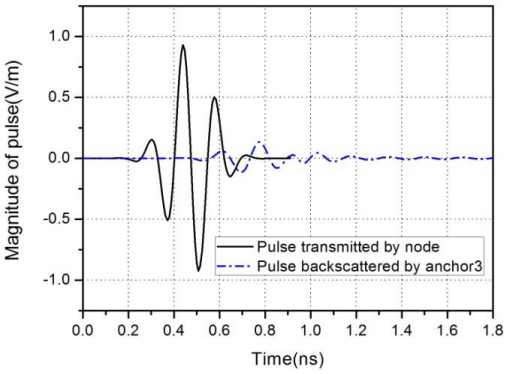

Fig. 8. Pulse backscattered by anchor3 compared with that transmitted by node.

Using the Equation (1) again, the coordinate of the node after calibration by time offset can be revised to (60.00542, 80.18034) mm. It is obviousness that, through the calibration, the deviation of the node in the horizontal direction is reduced to 0.00542mm, and the deviation in the vertical direction can be reduced to 0.18034mm simultaneously.

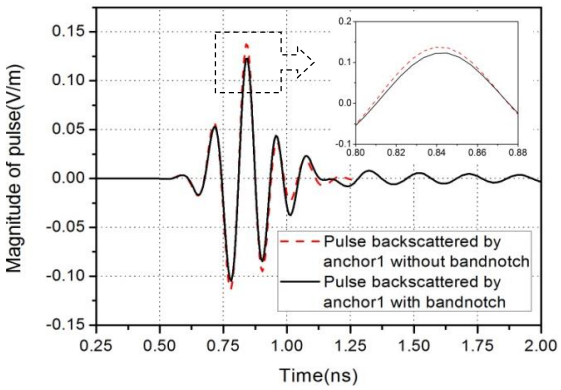

Fig. 9. Pulse backscattered by anchor1compared with that without band notch.

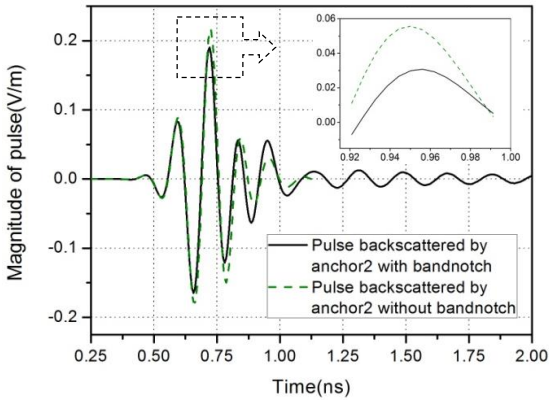

Fig. 10. Pulse backscattered by anchor2 compared with that without band notch.

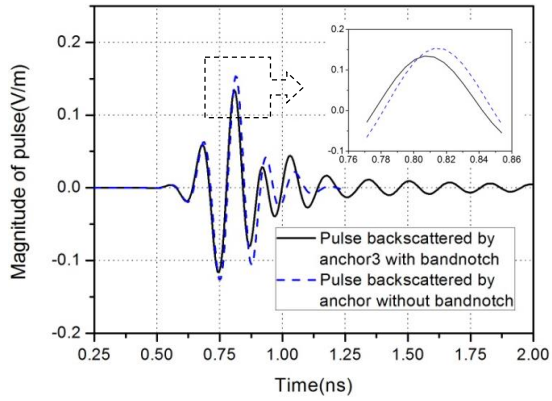

Fig. 11. Pulse backscattered by anchor3 compared with that without band notch.

V. CONCLUSION

According to the study in the paper, it can be concluded that compared with the narrow band circumstance, the IR-UWB is more effective in giving an accurate positioning, and the accuracy can be further improved by employing shorter, more precise pulses with higher level integrity. It is also concluded that the passive and chipless IR-UWB positioning is a simple and cost-efficient system. The positioning under this architecture can be implemented by recognizing not only the TOA of pulse but also the band-notch for anchor scrutinizing. Moreover, it can be concluded that the positioning deviation can be compensated by calibrating TOA with the time offset made by the pulses backscattered by the anchor with and without band-notch, respectively.

REFERENCES

[1] R. Bharadwaj, S. Swaisaenyakorn, C. G. Parini, et al., "Impulse radio-ultra wideband communications for localization and tracking of human body and limbs movement for healthcare applications," *IEEE Transactions on Antennas & Propagation*, vol. 65, no. 12, pp. 7298-7309, Dec. 2017.

[2] A. Alarifi, A. Al-Salman, M. Alsaleh, et al., "Ultra wideband indoor positioning technologies: Analysis and recent advances," *Sensors*, vol. 16, no. 5, article 707, 2016.

[3] S. Gezici, Z. Tian, G. B. Giannakis, H. Kobayashi, A. F. Molisch, H. V. Poor, and Z. Sahinoglu, "Positioning via ultra-wideband radios: a look at positioning aspects for future sensor networks," *IEEE Signal Process. Mag.*, vol. 22, no. 4, pp. 70-84, July 2005.

[4] D. Dardari, et al., "Ultrawide bandwidth RFID: The next generation?," *Proc. IEEE*, vol. 98, no. 9, pp. 1570-1582, Sep. 2010.

[5] R. J. Fontana, "Recent system applications of short-pulse ultra-wideband (UWB) technology," *IEEE Trans. Microw. Theory Tech.*, vol. 52, no. 9, pp. 2087-2104, Sep. 2004.

[6] M. S. Svalastog, "Indoor Positioning-Technologies, Services and Architectures," Cand. Scient. Thesis, University of Oslo, Oslo, Norway, 2007.

[7] C. C. Cruz, J. R. Costa, and C. A. Fernandes, "Hybrid UHF/UWB antenna for passive indoor identification and positioning systems," *IEEE Trans. Antennas Propag.*, vol. 61, no. 1, pp. 354-361, Sep. 2013.

[8] A. Chehri, P. Fortier, and P. M. Tardif, "UWB-based sensor networks for positioning in mining environments," *Ad Hoc Networks*., vol. 7, no. 5, pp. 987-1000, 2009.

[9] N. Decarli, F. Guidi, and D. Dardari, "Passive UWB RFID for tag positioning: architectures and design," *IEEE Sensors J.*, vol. 16, no. 5, pp. 1385-1397, Mar. 2016.

[10] L. Taponecco, A. A. D'Amico, and U. Mengali, "Joint TOA and AOA estimation for UWB positioning applications," *IEEE Trans. Wireless Commun.*, vol. 10, no. 7, pp. 2207-2217, July 2011.
[11] S. Hu, Y. Zhou, C. L. Law, and W. Dou, "Study of a uniplanar monopole antenna for passive chipless UWB-RFID positioning system," *IEEE Trans. Antennas Propag.*, vol. 58, no. 2, pp. 271-278, Feb. 2010.
[12] C. A. Balanis, *Antenna Theory: Analysis and Design*. 3rd edition, Wiley–Interscience, Hoboken, NJ, 2005.
[13] J. Liu and B. P. Li, "Palladium decorated SWCNTs sensor for detecting methane at room temperature based on UWB-RFID," *Applied Computational Electromagnetics Society Journal*, vol. 31, no. 8, pp. 989-996, Aug. 2016.
[14] A. Ramos, A. Lazaro, D. Girbau, et al., "Time-domain measurement of time-coded UWB chipless RFID tags," *Progress in Electromagnetics Research*, vol. 116, no. 8, pp. 313-331, 2011.
[15] Y. J. Cho, K. H. Kim, D. H. Choi, S. S. Lee, and S.-O. Park, "A miniature UWB planar monopole antenna with 5-GHz band-rejection filter and the time-domain characteristics," *IEEE Trans. Antennas Propag.*, vol. 54, no. 5, pp. 1453-1460, May 2006.
[16] K. Chung, J. Kim, and J. Choi, "Wideband microstrip-fed monopole antenna having frequency band-notch function," *IEEE Microw. Wireless Comp. Lett.*, vol. 15, no. 11, pp. 766-768, Nov. 2005.
[17] B. Tong, X. Wu, L. Xiao, et al., "Dual band-notched ultra-wideband antenna based on U-shaped slit and split ring slot," *Asia-Pacific Microwave Conference, IEEE*, pp. 1-3, 2015.
[18] CST Microwave Studio, ver. 2009, Computer Simulation Technology, Framingham, MA, 2009.

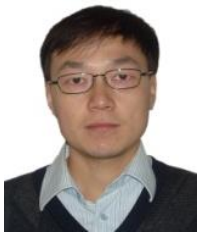

Jian Liu was born in Xi'an, Shaanxi, in 1967. He received the B.S. and M.S. degrees in the Electromagnetic Field Engineering from Xidian University, Xi'an, in 1990 and 1996. From 1990 to 1996, he was an Assistant Professor with the Communication Engineering Department, Xi'an Mining Institute. From 1997 to 1998, he was an Electrical Engineer with RF & Wireless Laboratory, ZTE. From 1998 to 2000, he was a Lecturer with the Communication Engineering Department, Xi'an Science and Technology College. From 2000 to 2003, he was the Senior Scientist and Project Leader with Philips Research Laboratory. From 2004 to 2010, he was Department head of PTCC, Panasonic Research and Development Cooperation Limited. Since 2010, he has been a Lecturer with the School of Communication and Information Engineering, Xi'an University of Science and Technology. He is the author of 1 text book, more than 10 articles, and holds 7 patents. His research interests include Computational Electromagnetism, Antenna, RF & Microwave Communication and Sensors.